Dynamic Modeling, Control and Simulation with Slip for an Omnidirectional Mobile Microrobot

Yiliang Jin, Jiapin Chen, and Zhenbo Li

Key laboratory for Thin Film and Microfabrication of Ministry of Education,
Institute of Micro/Nano Science and Technology, Shanghai Jiaotong University,
Shanghai 200240 China
snakeeking@gmail.com

Abstract. This paper investigates the nonlinear dynamic model of a millimeters-size omnidirectional mobile microrobot used for micro-assembly task, where the wheel/motion surface slip is considered. Some detailed factors are also taken into account for the micro size of the wheeled microrobot. Several dynamic simulation examples are presented here to demonstrate the deviation caused by the slip. After that, a vision feedback based control method is presented to reduce the deviation with the feedback of vision system.

Keywords: mobile microrobot, omnidirection, dynamics, slip.

1 Introduction

The microrobots based micro-assembly system is one of the main methods to solve micro-assembly problems in MEMS. A tri-wheeled mobile microrobot in this paper is designed to accomplish such assembly work. Therefore, the positioning precision of the microrobot appears to be extremely important and the work on the dynamic modeling also appears to be essential so as to improve the dynamic performance of it.

Modeling of wheeled mobile robots is generally described as nonholonomic dynamical system, in which the wheels are assumed to roll without slippage. However, the slippage actually exists during movement and it does affect the dynamic property of the wheeled microrobots and cause navigational error. Some researches have been reported on the investigation of dynamics with slip in mobile robots. Balakrishna presented a traction model considering of slip for the dynamic equation of the wheeled mobile robot[1]. Wiliams derives a nonlinear dynamic model for wheeled omnidirectional robots that includes slip between the wheels and motion surface[2]. Chung developed a dynamic model considering slip and incorporating Dugoff's tire friction model for a robotic manipulator mounted upon a wheeled mobile platform[3].

In this paper, the dynamic equations with slip for the wheeled microrobot are generated with the analysis of dynamics. And multiple detailed factors are taken into account while establishing the model due to the micro size of the robot. Without additional control method, the positioning performance shown by the simulation results appear to be somehow poor. So a vision feedback based control method is presented to reduce the deviation and improve the positioning performance.

C. Xiong et al. (Eds.): ICIRA 2008, Part I, LNAI 5314, pp. 911–920, 2008.
© Springer-Verlag Berlin Heidelberg 2008

Section 2 introduces the architecture of the wheeled mobile microrobot, including the mechanical structure and the control system. Section 3 establishes the dynamic model with slip, and makes the simulation. Section 4 presents a vision feedback based control method and simulations based on it, followed by conclusion.

2 System of the Omnidirectional Mobile Microrobot[4]

2.1 Tri-wheeled Omnidirectional Structure

The tri-wheeled mobile microrobot has a 9 mm×9 mm×9.8mm size as shown in Fig. 1(a) and weighs 2.8g. The robot is composed of three wheels mutually geared through three big microgears and one small microgear with 3:1 transmission ratio, and a piezoelectric microgripper, as shown in Fig. 1(b). Four 3mm electromagnetic micromotors are applied to actuate the robot.

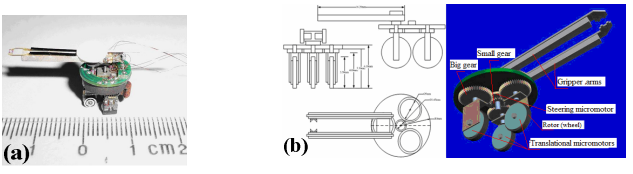

Fig. 1. The tri-wheeled millimeters-size mobile microrobot. (a) side view of the microrobot. (b) the CAD model diagram of the microrobot.

Connected by the gear set, during the rotational movement, the three wheels can steer synchronously in the same angle. This structure also can make translational movement and rotational movement separately, thus to achieve the omnidirectonal movement.

2.2 The System for Assembly Task

The control system of the tri-wheeled mobile microrobot consists of two platform, two cameras for image capture (one for macro platform with supervised area 15cm×15cm, one for micro platform with supervised area 2mm×2mm), a host computer and a control PCB as shown in Fig. 2. The vision system with cameras can capture the current position of the robot in the platforms and send back the position

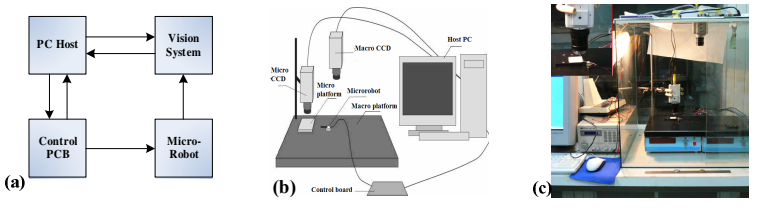

Fig. 2. The system for assembly task. (a) the frame for the system. (b) the CAD model of the system. (c) the photo of the system.

information to host computer. Based on the feedback from the vision system, the computer can determine the next action of the robot and derive proper control method.

In this paper, our prime purpose is to control the robot to move from current location to goal location precisely. Thus it can move to the micro-work platform accurately so as to complete the micro-assembly task effectively. Slip in the motion is a main factor to affect the dynamic performance of the microrobot. Therefore, it is essential to analyze the slip problem and find an effective way to solve it.

3 Dynamic Modeling

In this section, the dynamic model of the wheeled mobile microrobot with slip is presented. And some simulation examples based on this model are executed.

3.1 Model of Slipping Velocity

Fig. 4(a) shows the top view of the tri-wheeled mobile microrobot model without the gripper. Since all the actions of the microrobot are performed on a plane, a planar coordinate system is used to analyze the dynamic model. The inertial frame is $\{O\}$, and the robot frame, i.e. the moving frame, settled on the center of the chassis of robot is $\{M\}$. The three wheels are symmetrically placed, aligned by 120° from each other, and the center of each wheel is fixed with respect to the robot frame. The distance from the center of each wheel to the origin of $\{M\}$ is defined as L. The orientation of the robot with respect to the inertial frame horizontal direction X_0 is given by angle φ.

As shown in Fig. 3(b), the unit vector $\overrightarrow{W_k}$ and $\overrightarrow{T_k}$ that is perpendicular to $\overrightarrow{W_k}$ present the instantaneous lognitudinal and transverse direction of each wheel, respectively. The angle from $\overrightarrow{X_M}$ to the lognitudinal direction is denoted as θ_k.

Fig. 4 shows the front view of the wheel, G is the contact point between the wheel and ground. With the non-slip constraint, in both lognitudinal and transverse direction, the velocity on the point G should add up to be zero[5]. It can be written as,

$$\overrightarrow{V_r^o} + \overrightarrow{V_\varphi^o} + \overrightarrow{V_{wk}^o} = 0, \quad k = 1,2,3. \tag{1}$$

$$\overrightarrow{V_r^o} = \begin{pmatrix} \dot{x}^o & \dot{y}^o & \dot{z}^o \end{pmatrix}^T, \overrightarrow{V_\varphi^o} = \overrightarrow{\dot{\varphi}^o} \times \overrightarrow{L_k^o}, \overrightarrow{V_{wk}^o} = \overrightarrow{\dot{\phi}_k^o} \times \overrightarrow{r_k^o}, \quad k = 1,2,3. \tag{2}$$

where $\overrightarrow{V_r^o}$ is the translational velocity of the robot center of mass, $\overrightarrow{\varphi^o}$ is the rotational velocity of the wheeled robot, $\overrightarrow{\dot{\phi}_k^o}$ is the angular velocity of the kth wheel, and $\overrightarrow{r_k^o}$ gives the wheel center position. The vectors are all with respect to the inertial frame.

When considering of the sliding motion, denoting the slipping velocity $\overrightarrow{V_{Sk}}$ as

$$\overrightarrow{V_{Sk}^o} = \overrightarrow{V_r^o} + \overrightarrow{V_\varphi^o} + \overrightarrow{V_{wk}^o}, \quad k = 1,2,3. \tag{3}$$

The lognitudinal component of the slipping velocity V^o_{SLk} and the transverse sliding velocity component V^o_{STk} can be obtained by the dot products between $\overline{V^o_{Sk}}$ and $\overline{W_k}$, $\overline{V^o_{Sk}}$ and $\overline{T_k}$, respectively:

$$V^o_{SLk} = \overline{V^o_{sk}} \bullet \overline{W^o_k} = (\overline{V_r{}^o} + \overline{\dot{\varphi}^o} \times \overline{L^o_k} + \overline{\dot{\phi}^o} \times \overline{r^o_k}) \bullet \overline{W^o_k}, \quad k = 1,2,3 . \tag{4}$$

$$V^o_{STk} = \overline{V^o_{sk}} \bullet \overline{T^o_k} = (\overline{V_r{}^o} + \overline{\dot{\varphi}^o} \times \overline{L^o_k} + \overline{\dot{\phi}^o} \times \overline{r^o_k}) \bullet \overline{T^o_k}, \quad k = 1,2,3 . \tag{5}$$

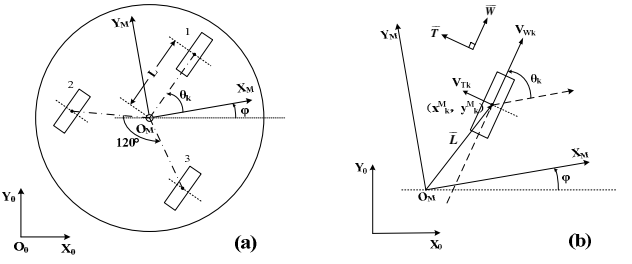

Fig. 3. Model of the wheeled mobile microrobot. (a) top view of the robot model. (b) top view of the one wheel model. (c).

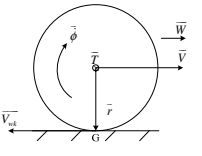

Fig. 4. The front view of the wheel

Orthonormal rotation matrix ${}^O_M R$ is used to convert the position vectors and unit direction vectors in robot frame to inertial frame[5],

$${}^O_M R = \begin{pmatrix} \cos\varphi & -\sin\varphi & 0 \\ \sin\varphi & \cos\varphi & 0 \\ 0 & 0 & 1 \end{pmatrix}. \tag{6}$$

$$\overline{W^o_k} = {}^O_M R \cdot \overline{W^M_k}, \overline{T^o_k} = {}^O_M R \cdot \overline{T^M_k}, \quad k = 1,2,3 . \tag{7}$$

where $\overline{W^M_k} = \begin{pmatrix} \cos\theta_k & \sin\theta_k & 0 \end{pmatrix}^T$, $\overline{T^M_k} = \begin{pmatrix} -\sin\theta_k & \cos\theta_k & 0 \end{pmatrix}^T$.

Therefore, (4) and (5) can be written as,

$$V^o_{SLk} = [\overline{V_r{}^o} + \overline{\dot{\varphi}^o} \times ({}^O_M R \cdot \overline{L^M_k}) + \overline{\dot{\phi}^o} \times ({}^O_M R \cdot \overline{r^M_k})] \bullet ({}^O_M R \cdot \overline{W^M_k}), \quad k = 1,2,3 . \tag{8}$$

$$V^o_{STk} = [\overline{V_r{}^o} + \overline{\dot{\varphi}^o} \times ({}^O_M R \cdot \overline{L^M_k}) + \overline{\dot{\phi}^o} \times ({}^O_M R \cdot \overline{r^M_k})] \bullet ({}^O_M R \cdot \overline{T^M_k}), \quad k = 1,2,3 . \tag{9}$$

3.2 Model of Friction

Friction plays an important role in robot manipulator simulations, and it is a prime factor affecting the dynamic property of the wheeled robot.

The difficulty with modeling friction is the complexity of the phenomenon at low velocity and, in particular, of the stick-slip process[6].One extensively-used model is the classical Coulomb model, but its discontinuity at zero may cause instability in simulation. Thus, in this research, another simplified model[2] is used for the coefficient of friction as shown in Equ. 10,

$$\mu(V_S) = \mu \frac{2}{\pi} \operatorname{atan}(pV_S) . \tag{10}$$

where V_S is the slipping velocity, μ is the static friction coefficient.

This continuous function can avoid algorithmic problems during the simulation, and it also fits the property of friction—the friction reduces as the slip reduces. p is a constant to modify the curve on its steepness and it is chosen as 1000 to approach the real condition in this paper. Here assuming that static friction coefficient equal to the dynamic friction coefficient between the rubbing surfaces and the weight of the robot is distributed averagely, then the friction on point G can be denoted as,

$$\overrightarrow{F_k^o} = -\frac{mg}{3}[\mu_L(V_{SLk}) \cdot ({}_M^O R \cdot \overrightarrow{W_k^M}) + \mu_T(V_{STk}) \cdot ({}_M^O R \cdot \overrightarrow{T_k^M})] . \tag{11}$$

where $\mu_L(V_{SLk})$ and $\mu_T(V_{STk})$ are the function for longitudinal and transverse friction coefficient versus the relative slipping velocity, respectively.

3.3 Additional Torque

As illustrated in Fig. 5, wheel1 is supported with a single-side cantilever while wheel2 and wheel3 are connected with the gear on the chassis through double-side cantilever. The asymmetry of single-side cantilever raises an additional torque T_a (see Equ. 12) that will cause unwanted rotation during the translational motion,

$$\overrightarrow{T_a^o} = \overrightarrow{d_1^o} \times \overrightarrow{F_1^o} = ({}_M^O R \cdot \overrightarrow{d_1^M}) \times \overrightarrow{F_1^o} . \tag{12}$$

where d_1 is the distance between the center of the wheel and the cantilever.

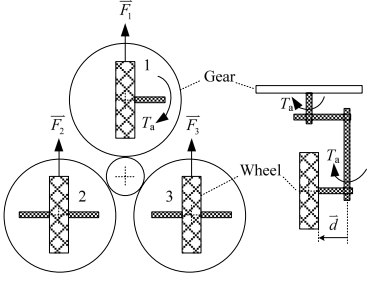

Fig. 5. The asymmetry of the supporting structure of wheel1 causes additional torque

3.4 The Dynamic Model with Slip

Within the above analysis and rigid body dynamics, the dynamic equations with slip can be concluded as follow,

$$\left\{\begin{array}{l} m\ddot{x}^o = \sum_{k=1}^{3} \overline{F_k^o} \bullet \overline{X^o} \\ m\ddot{y}^o = \sum_{k=1}^{3} \overline{F_k^o} \bullet \overline{Y^o} \\ I\ddot{\varphi}^o = \sum_{k=1}^{3} [({}_M^O R \cdot \overline{L^M}) \times \overline{F_k^o}] \bullet \overline{Z^o} + \overline{T_a^o} \bullet \overline{Z^o} \end{array}\right\}. \tag{13}$$

where $\overline{X^o}$, $\overline{Y^o}$, $\overline{Z^o}$ are the unit vectors of the axles of the inertial coordinate, I is the moment of inertia of the microrobot, and as the chassis is shaped as a circle and wheel weighs much less, I can be obtained by $I = \frac{1}{2} mR^2$.

3.5 Initial Simulations

In initial simulation, to make the slip phenomenon obvious, the microrobot is manipulated without additional control method: calculating the θ and time t according to the goal location, initial location and stable wheel angle velocity, then let the microrobot move in θ direction for t s. The stable velocity of the microrobot is set as 8.7 rad/s, the wheel acceleration and deceleration are set as 50 rad/s^2, -50rad/s^2, respectively, and φ is initialized as 0°. The other dynamic parameters are given as follow: m=2.8g, μ_L=μ_T=0.21, L_1=L_2=L_3=4.15mm, r_1=r_2=r_3=1.65mm, d_1=1mm. In the simulation, the steering action is assumed to be accurate. All the simulations are conducted in Matlab based on the dynamic model presented previously.

3.5.1 Simulation for Different States of Wheel1

To simplify the structure, it has been considered that to equip wheel1 without micromotor, and to use it as a passive wheel. To verify the feasibility, a simulation is conducted. The robot with wheel1 in active state or passive state respectively is manipulated to move for 14.355mm with different direction angle. The simulation result is shown in Fig. 6 which presents that while using wheel1 as a passive wheel, the drift from the goal location is much larger compared to that while wheel1 is an active wheel. As the wheel1 in passive state affects the dynamic performance in some extent, wheel1 remains its active state in the following researches.

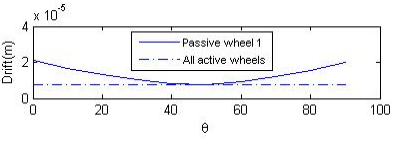

Fig. 6. Simulation for the state of wheel1 (drift from the goal versus the direction angle θ)

3.5.2 Simulation for the Assembly Error of Wheels

Because the size of the microrobot is too small, it is too difficult for any machine to assemble it automatically. Therefore, the microrobot is assembled all by hand and as a result, the error on the assembly definitely exists. These assembly errors among the wheels are hardly observed by eye, but actually affect the dynamic property a lot. Assuming that the three wheels all are active wheels, wheel1 is assembled accurately, wheel2 and wheel3 have the same offset angle ξ from wheel1 ranging from -10°to 10°,trajectory is set from location $(0\ 0\ 0)^T$ to $(10.15\ 10.15\ 0)^T$ (mm). As shown in Fig. 7, the simulation result presents that as ξ deviates from zero, the drift grows up.

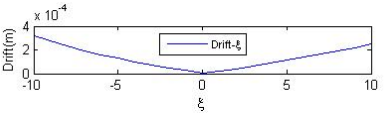

Fig. 7. Simulation for the error in assembly (drift from the goal versus the offset angle ξ)

3.5.3 Simulation for Translational Movement

As analyzed above, in translational movement simulation, all the factors affecting the dynamic property should be considered. The wheels are all assumed to be active and, wheel2 and wheel3 align by 3°and 2°from wheel1, respectively. The trajectory is set from location $(0\ 0\ 0)^T$ to $(28.71\ 0\ 0)^T$ (mm) specifying the moving time as 2s and the direction angle $\theta = 0^\circ$. Other conditions are same as mentioned above.

The simulation result is shown in Fig. 8. Fig. 8(a) and Fig. 8(b) show the lognitudinal and transverse slipping velocity of the three wheels, respectively. Because of the high acceleration and deceleration, the assembly error of the three wheels, and the additional torque, the slippage exists during the whole process. The simulation route and the ideal route of the microrobot are both shown in Fig. 8(c). The stop location

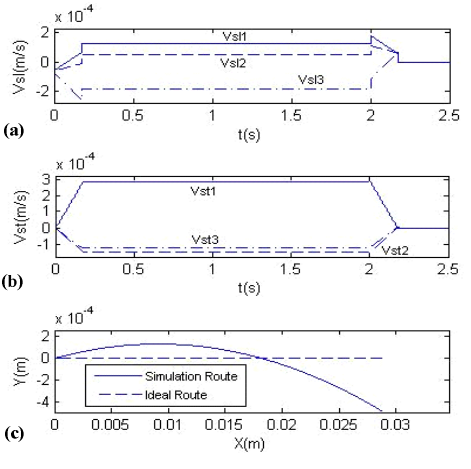

Fig. 8. The results for the translational movement simulation. (a) lognitudinal slipping speed versus time. (b) transverse slipping speed versus time. (c) the simulation route compared to the ideal route with the moving distance of 28.71mm.

has a 0.4727mm drift from the goal which is small but also should be taken into account for the microrobot. With the above results, it can be fingered out that as the route increases, the deviation of positioning will present a large increment.

4 Vision Feedback Based Control Method

With the above simulation results, it can be found that the microrobot would drift far away from the goal location as the moving route increases without additional control method. In this section, a vision feedback based control method is presented to improve the positioning performance for the wheeled microrobot.

4.1 The Principle of the Vision Feedback Based Control Method

In this control system, CCD cameras are used to supervise the wheeled mobile microrobot and locate it in the platform. The cameras are just used as a measure tool while using no additional control method. To improve the performance of the positioning of the microrobot, the location data obtained by the vision system is used as feedback and a close-loop control system is established.

The diagram of the proposed control system is shown in Fig. 9. The control method is written into the maneuver controller of the control PCB. As the goal location is determined, the initial moving direction can be set and the microrobot will be activated. Since that the sensitivity of the vision system is not high enough to work in real-time mode during the moving action of the microrobot, the robot need to be in stationary state while capturing the position of it. The movement from initial location to goal location is separated into many short periods--stop the robot after every period, capture, then modify the direction and maneuver. Two timers are designed for count the time. Timer1 is used for controlling the moving time of the microrobot and set by the maneuver controller. Timer2 set as 0.1s in this paper waits for the stop of slip.

After stopping the micro-robot in every period, the vision system captures the position of the robot and gives a feedback to the angle modifier and the distance comparator on the control PCB. Using the data transmitted from the vision system, the angle modifier will modify the direction θ_1 to make the moving direction of the robot align towards the goal location. The modified angel is denoted as θ_1',

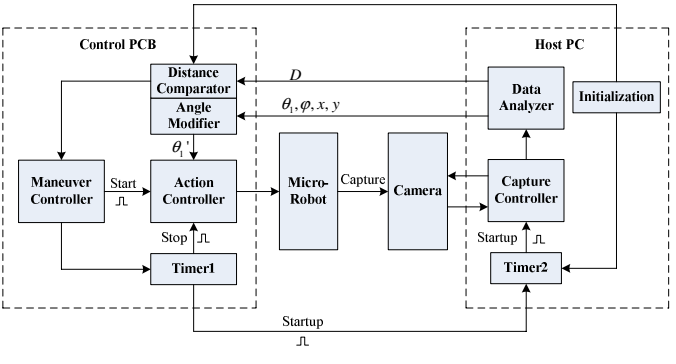

Fig. 9. Diagram of the work principle of the vision feedback based control system

$$\theta_1' = \alpha - \varphi \,. \tag{14}$$

Where α is the angle from $\overline{X_o}$ to the modified direction $\overline{Goal}$ as illustrated in Fig. 10.

The distance comparator compares the distance from current location to goal location to the settled value initialized as 2mm in this paper. If the former is larger, the maneuver will receive the information to set the value of timer1 to 0.2s. Otherwise, the timer1 would be set as 0.05s to limit the moving distance of each period.

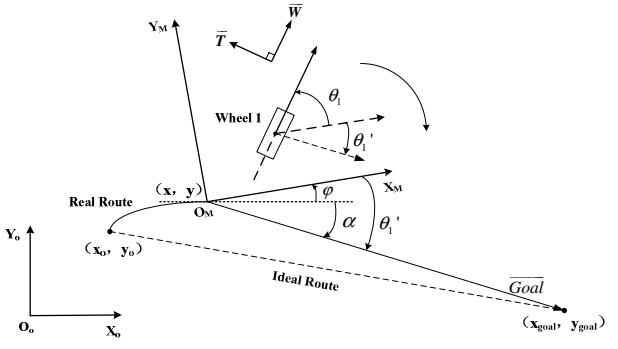

Fig. 10. Modify the direction angle θ_1 in each period of movement

4.2 Simulation Result

Based on the vision feedback based control method, a new translational movement simulation is made in this section. To observe the slippage effect obviously, the trajectory is set from location $(0\ 0\ 0)^T$ to $(100\ 0\ 0)^T$ (mm) specifying the moving time as 7s and the initial direction angle $\theta = 0^\circ$.

The simulation result is shown in Fig. 11. It can be clearly observed that the microrobot drifts far away from the designed route at last without additional control method, the deviation reaches 13mm. While using the vision feedback based control method, the microrobot moves in a smooth route and achieves the work much better, the deviation is only 0.0124mm which affects the positioning work much less.

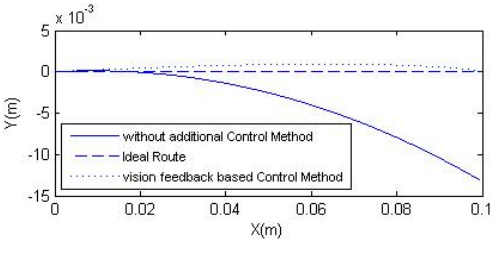

Fig. 11. The result for the translational movement simulation with vision feedback based control method compared to that without additional control method

5 Conclusion and Future Work

In this paper, a dynamic model incorporated the effects of slip is presented for the tri-wheeled millimeters-size mobile robot. The dynamic model contains multiple factors that influence the dynamic property of the wheeled microrobot. With the simulations, it is shown that slip affects the dynamic property of the microrobot significantly.

Without additional control method, the simulations indicated that the deviation would grown up, giving a bad performance of positioning as the moving distance increased. Therefore, a vision feedback based control method was presented to meliorate the dynamic performance. And following simulation showed that the drift appeared to be much less under the vision feedback based control method. And the future work based on this microrobot would be to establish dynamic model including the steering motion and other factors which is idealized in current research.

Acknowledgements

This work is supported by Hi-Tech Research and Development Program of China (No. 2007AA04Z340), and Specialized Research Fund for the Doctoral Program of Higher Education of China (No.20060248057).

References

1. Balakrishna, R., Ghosal, A.: Modeling of Slip for Wheeled Mobile Robots. IEEE Transactions on Robotics and Automation 11, 126–132 (1995)
2. Williams II, R.L., Carter, B.E., Gallina, P., Rosati, G.: Dynamic Model With Slip for Wheeled Omnidirectional Robots. IEEE Transactions on Robotics and Automation 18, 285–293 (2002)
3. Chung, J.H., Velinsky, S.A.: Robust Interaction Control of a Mobile Manipulator-Dynamic Model Based Coordination. Journal of Intelligent and Robotic Systems 26, 47–63 (1999)
4. Li, J., Li, Z., Chen, J.: An Omni-directional Mobile Millimeter-sized Micro-robot with 3-mm Electromagnetic Micro-motors for a Micro-factory. Advanced Robotics 21, 1369–1391 (2007)
5. Craig, J.J.: Introduction to Robotics: Mechanics and Control. Addison-Wesley, Boston (1989)
6. Piedb, J.-c., Hurteau, R.: Friction and Stick-Slip in Robots: Simulation and Experimentation. Multibody System Dynamics 4, 341–354 (2000)